

Brachiating Robot Analysis and Design

ElHussein Shata

Department of Mechanical Engineering
South Dakota State University
Brookings, SD
elhussein.shata@sdstate.edu

Praneel Acharya

Department of Mechanical Engineering
South Dakota State University
Brookings, SD
praneel.acharya@sdstate.edu

Kim-Doang Nguyen

Department of Mechanical Engineering
South Dakota State University
Brookings, SD
doang.nguyen@sdstate.edu

Abstract – A robot with the ability to brachiate could prove to be very useful in reducing the number of work related accidents due to falling from high altitudes or maintenance of high voltage towers. It could also help a company's bottom line by reducing the number of workers required to accomplish a task. In addition, it can be used to scale lattice structures for inspection. Inspired by nature, gibbons prove to have the best pendulum like motion and power to weight ratio.

In this paper, we investigate the mechanics of gibbons and try to simplify its dynamics by a mechanical system. A simple way to characterize the motion of a gibbon is a two-bar linkage controlled by one motor. It has proven that this mechanism can achieve a good power to weight ratio and can approach the desired motion. By exploiting this motion, the device can create its own momentum to swing, and utilizing a system of grippers to grab and release members, will have the ability to navigate any structure. Furthermore, outfitting these robots with inspection tools such as cameras could allow the inspection of transmission towers and bridges safer, easier, and quicker. The hands-on approach of a mechanism like this could also accomplish tasks that may prove to be too dangerous or difficult for drones to accomplish.

Keywords—brachiators, two-bar linkage

I. INTRODUCTION

Robots have been emerging rapidly in daily lives in the past decades. As technology advances, robots have enabled humans to live more convenient lives [1]. More importantly, robotic technology allows us to decrease the loss of human lives due to dangerous working conditions [2].

According to the U.S. Department of Labor, falls are one of the leading causes of death for workers while on the job [3]. In 2015, falls accounted for nearly 17% of the total workplace deaths. Secondly, the federal government is notoriously understaffed when it comes to infrastructure inspection [4]. A device that can increase the efficiency of an inspection or reduce the number of workers needed to complete inspection will save tax dollars and possibly human lives.

Currently, drones are being utilized and outfitted with cameras and other hardware to make inspecting quicker and easier [5]. However, the use of these drones has its own drawbacks. One issue is that drones could have problems navigating tight lattice structures resulting in a size concern. Another issue is the fact that system failures and damage will almost certainly end in complete destruction of the device due to the structural requirements for flying and the heights the drone will be working at. To remedy these concerns, a robot that can swing from a member to another in a lattice structure can be more durable than a drone and prove to be effective at aiding in infrastructure inspection and scaling lattice structures.

II. CONCEPT

Inspired from nature, gibbons are the finest animals that swings and generate pendulum like motion [6]. With the capability to produce the best power-to-weight ratio and perfect centralized mass distribution, gibbons brachiate with a very low mechanical cost. The closer the design comes to achieving this power to weight ratio the more efficient the design will be able to accomplish its task. The pendulum-like motion gibbons use to build up moment for a swing by kicking its legs can be replicated in a device that can use a similar concept to build up its own momentum and achieve alike motion [7].

Upon studying gibbons, their upper body is found to be a five-bar linkage [8] with the ability to grab and release surfaces using their hands, as illustrated in Figure 1. Although a five-bar linkage would be ideal to represent a gibbon's biomechanical body, it requires unnecessarily large number of freedoms, which in turn implies a large number of actuator required to drive the robot. This dramatically complicate the controls of the robot [9,10].

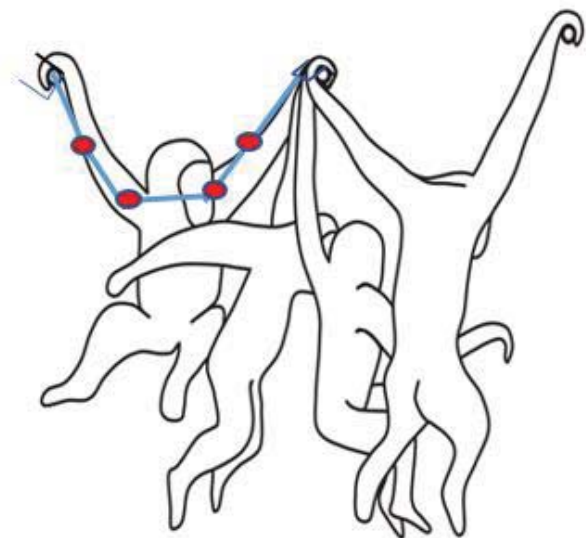


Figure 1: Five-bar linkage illustration

To address this problem, we employ a two-bar linkage mechanism that will reduce the complexity and weight of the mechanism, making the system easier to control and more applicable to use. It is similar to the mechanism in [11], which use a variable stiffness actuator with two motors. In contrast, here, we only design one actuating input at the elbow joint for swinging. Once successful swinging motions are achieved, the robot can brachiate among a rope or a lattice structure like bridges or transmission towers.

In addition, in order for the robot to reach more places and maneuver around corners, a motor is added at the end of each arm to create a wrist joint and to ensure the dexterity of turning in any structure. As shown in Figure 2, the brachiator mechanism is introduced with the wrist motion that allows each linkage to turn 180°. A set of two gears with identical number of teeth and pitch diameter are added at the joint to increase the stroke angle by allowing us to move the driving motor away from the joint. In addition, it ensures the force transmission with minimal energy loss.

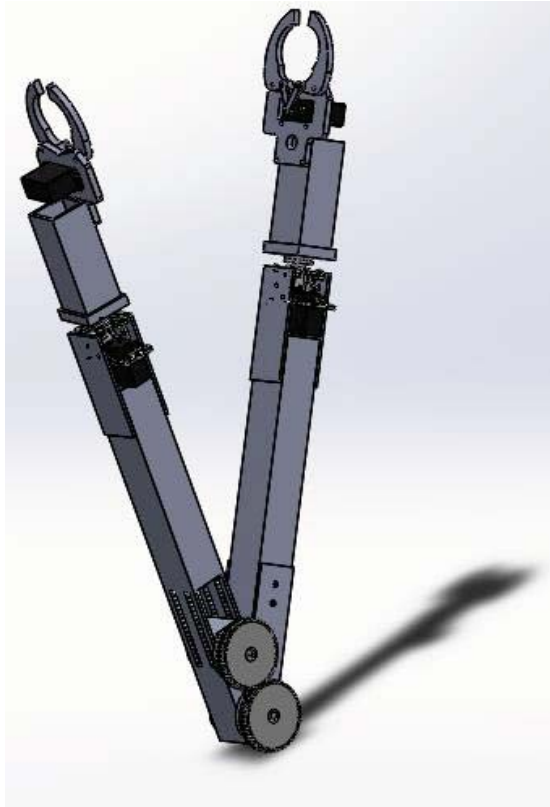


Figure 2: Proposed design

To reduce the weight and avoid adding any counter balance deadweight, the motor is inserted in one of the links. By mounting the motor within the frame, the brachiator would be more stable since the motor's center of mass will be close to that of the frame's center of mass.

A gripper is added to the end of each link in order to ensure grasping and releasing surfaces. Each gripper is composed of a pair claw-like pieces driven by a servo motor. The motor used in each of the gripper's mechanism is HS-422 servomotor with torque of 57 oz-in which is tested to be enough to hold the system.

The wrist mechanism added to the design consists of a servomotor in a case that is mounted to a bearing. As a result, the body of the servomotor and the output shaft will rotate in different axis. The mechanism increases the servo's load-bearing capabilities by helping to isolate the lateral load from the servo spline and case. A three-dimensional model for the wrist mechanism is shown in Figure 3 below.



Figure 3: Wrist mechanism CAD

III. MOTOR TORQUE CALCULATION

To anticipate the right value of torque needed per swing, a free fall calculation is performed on one linkage of mass of 0.6732 kg. We first calculate the expected velocity of one arm linkage as illustrated in Figure 4

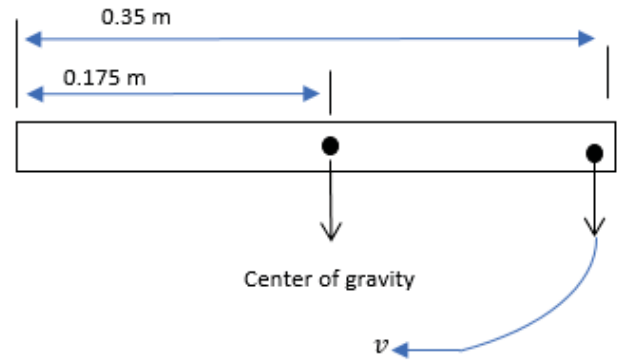


Figure 4: Velocity analysis

Kinetic Energy = Potential Energy

$$\begin{aligned}
 \frac{1}{2}mv^2 &= mgh \\
 \frac{1}{2}v^2 &= gh \\
 v &= \sqrt{2gh} \\
 v &= \sqrt{2 \left(9.81 \frac{m}{s^2}\right) (0.175 m)} \\
 v &= 1.8529 \frac{m}{s}
 \end{aligned} \tag{1}$$

Next, we calculate the angular velocity of the link:

$$\begin{aligned}
 \omega &= \frac{v}{R} = \frac{1.8529}{0.175} \\
 \omega &= 10.588 \frac{rad}{sec} \\
 \omega &= 101.12 rpm.
 \end{aligned} \tag{2}$$

Therefore, the torque required is:

$$\begin{aligned}
 \tau &= Fd \\
 \tau &= mgd \\
 \tau &= (0.6732 kg) \left(9.81 \frac{m}{s^2}\right) (0.175 m) \\
 \tau &= 1.155 N - m \\
 \tau &= 163.56 oz - in.
 \end{aligned} \tag{3}$$

TABLE 1
TORQUE, CURRENT, AND SPEED DATA

	8 Volt			10 Volt		12 Volt	
Weight (lb.)	Torque (lb.in)	Current (A)	Speed (rpm)	Current (A)	Speed (rpm)	Current (A)	Speed (rpm)
0.806892	0.476510877	0.3	83.3	0.27	104.6	0.37	126.2
1.356892	0.801313927	0.31	69.7	0.32	102.5	0.42	122.6
1.806892	1.067061877	0.39	76.2	0.38	99.9	0.39	122
2.356892	1.391864927	0.46	74.5	0.44	98.2	0.46	120
2.806892	1.657612877	0.52	71.4	0.54	93.3	0.57	117
3.806892	2.248163877	0.65	67	0.67	90.4	0.72	108.4
4.806892	2.838714877	1.4	52	0.8	80.6	0.94	105.4

Multiplying the torque value by a safety factor gives $\tau = 163.56 \text{ oz-in} \times 4 = 654.24 \text{ oz-in}$. This means we need a motor that can produce a minimum of 654.24 oz-in of stall torque.

IV. MOTOR EXPERIMENT

To validate the calculated values of the motor, this section discusses an experimental process to systematically select the motor. Another purpose for testing different motors was to study the motor's torque behavior versus current and to validate that any motor that has a torque below the calculated torque in Equation (3) will not be a valid selection. An initial experiment took place by testing a DC motor with a stall torque of 120 oz-in, and a speed of 130 rpm. The experimental set-up shown in Figure 5. A mounting hub is connected to the DC motor's shaft, a rubber grommet that is mounted on the shaft, and a polypropylene string that is tied around the rubber grommet. A weight holder is then tied at the bottom of the string with different weights. A tachometer is used to record the angular velocity of the motor while a load is being added

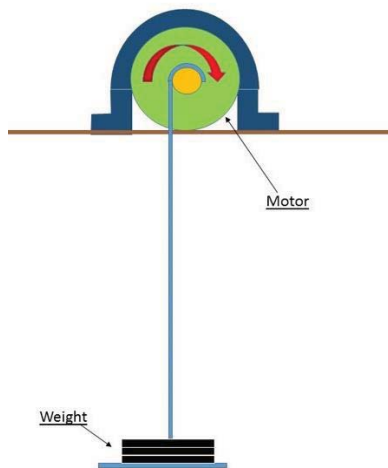


Figure 5: Experimental setup

equation $\tau = F \cdot d$. Where F is the weight added, and d is the radius of the spool plus the rubber grommet.

Table 1 shows the data collected during the experiment. For each run, weight and voltage were increased gradually with a careful consideration to the maximum voltage the motor can take, and that is 12V. The speed of the motor was recorded during each run and a torque calculation was then performed based on the collected data.

The maximum weight the DC motor was able to lift was 4.8 lb. Free run speed from the Manufacturers specifications at 12 Volts is 130 rpms. The speed measured during the experiment came close to 130 rpm when the DC motor was given 12 Volts and before adding any weights, and that proves that the collected results are dependable.

The inversely proportional relationship between the torque and speed can be seen in the Figure 6. As expected, increasing the weight applied on the motor, increases the torque, which in turn decreases the rotational speed of the motor.

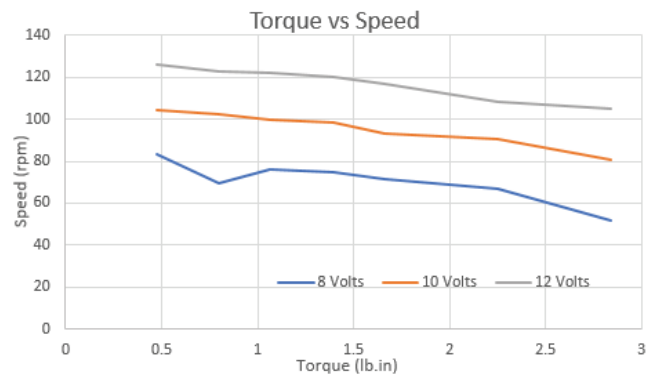


Figure 6: Torque vs Speed plot

Based on the measured data, Figure 7 shows the relationship between the calculated torque and the measured current. It has proven that the output torque is directly proportional to the drawn current. Depending on the performed experiment, as torque increases, current drawn to the motor also increases.

For each weight added, different voltages were supplied to the motor. The current and angular velocity were recorded during the experiment. Torque was calculated using the

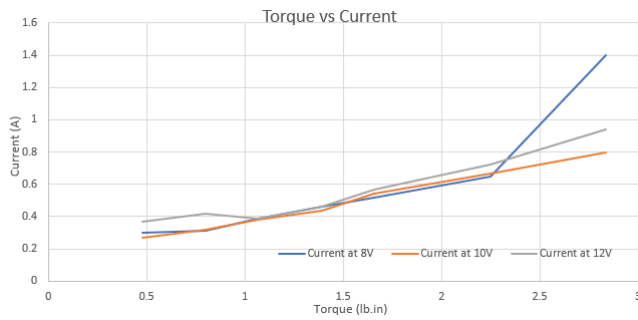


Figure 7: Torque vs Current plot

Before coming down to the right value of the torque needed, three different motors with different torque values were experimented. The first one electrically failed due to the high load on the motor shaft which drawn high current from the power source. The second one mechanically failed due to the shear stress created on the gears inside the gearbox which broke the gears teeth.

The last one was the most suitable motor found to produce the amount of torque and speed needed in the next section. It is a planetary gear motor with stall torque of 680 oz-in and a maximum shaft speed of 165 rpm.

Testing the DC motor proves the theory behind the torque's relationship with the current to be true. Calibrating the torque produced by the motor gives more insight into how much torque will be needed to operate a successful brachiating motion. Through analyzing the collected data, a better understanding on the maximum velocity that the motor can achieve under different loading conditions was obtained. In addition, we verified the right value of the motor's torque selection.

V. FABRICATION

Based on our experiments and calculations, the selected motor has a stall torque of 680 oz-in and a shaft speed of 165 rpm. By adding gears at the joint as shown in Figure 8, the speed of the motor is ensured to transmit from one arm to the other. The gears used are made from aluminum and have characteristics of 84 teeth, an outer diameter of 2.688 inches, and a bore of 0.5 inches.

A hand mill was used in the initial fabrication but the accuracy of the hand mill was not good enough to apply the dimensions and align the two gears together. A CNC machine was then used to precisely drill the two holes, one for the motor and one for the bearings. A G-Code was developed based on the proposed design to produce the arm linkage. It was fabricated successfully, and the two gears fit nicely.

The joints are connected together with a $\frac{1}{2}$ " aluminum shaft and welded on both sides to ensure permanent fix. Two bearings are added on each side of the shaft to separate the motion of the arms, so they can move freely with no constrain to each other.

The robot is made from aluminum 6063 rather than 6061 because it is lighter and softer in fabrication. With yield strength of 16,000 psi and hardness of 55 Brinel, which give a good combination of high strength and machinable aluminum [12].

Figure 8 shows the fabricated brachiator in a stationary position holding onto a bar that is wrapped with rubber. The rubber is used to ensure a friction surface between the gripper and the bar.

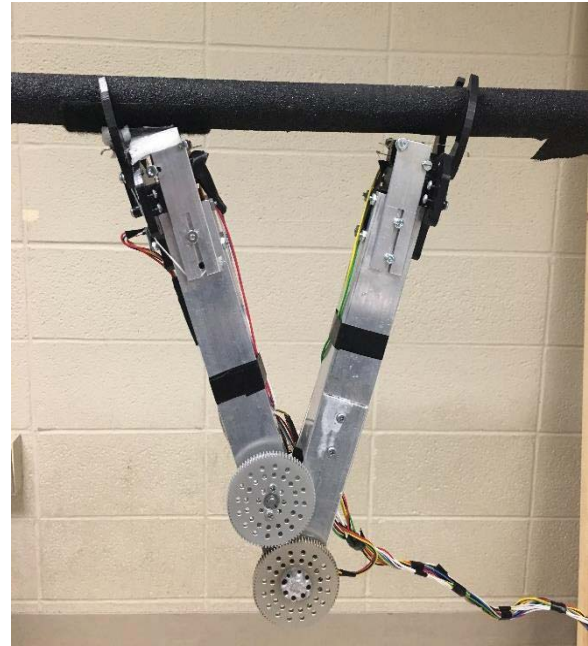


Figure 8: Fabricated mechanism

Figure 9 demonstrate a full span of the brachiator with one gripper holding onto the bar as a part of testing the motor and initial control algorithm.



Figure 9: Full span illustration

The fabricated wrist mechanism for changing axes is shown in Figure 10. The wrist mechanism was initially fabricated with polylactide (PLA) by using a three-dimensional printer. However, the material proved to be not strong enough to hold the entire arm and failed after a few swings.

Another version of the wrist case will be made from aluminum 6061 that will allow the frame to withstand more load [13] while avoiding material fracture or failure. The frame will act as the servo exoskeleton and it will greatly enhance the mechanical loads that the servo and the brachiator can withstand. The designed frame will have repeated pattern throughout the case to allow endless attachment options and insure arm's security and stiffness while brachiating.

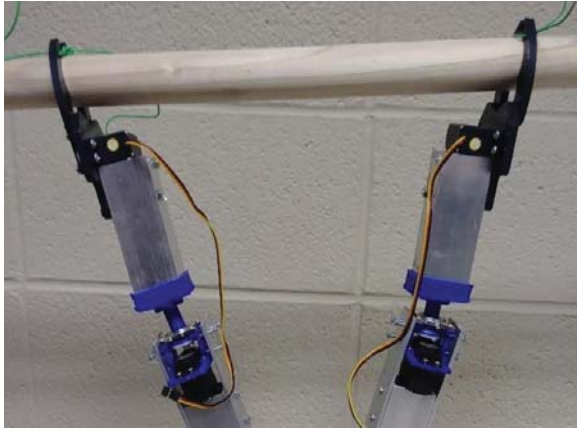


Figure 10: 3D printed wrist mechanism

VI. MECHANISM TESTING

After fabricating the robot, a wooden frame was built with a testing net bed at the bottom to avoid the drop crash while testing. A grip tape was wrapped around the grip bar to increase friction between the gripper and the wooden surface.

An Arduino was used in testing and control, a motor driver L298N was added in between the DC motor and power source to ensure a sink for the voltage heat, and avoid frying the motor's circuit. An encoder is attached to the backside end of the DC motor's shaft to locate the shaft's position and use it to identify the location for one of the arms. An IMU6050 was added to the other arm to localize its position and use it as a feedback for the grippers to close.

To ensure safety, two bump sensors were added at the joint to avoid hitting the motor while closing the arms. A bump sensor was also added in the grippers to sense the rod when it touches it in case of an electric failure.

VII. CONCLUSION

In summary, this paper analyzes the behavior and design of a bio-inspired mechanism that can be mimicked with a two-bar linkage, as a simple way to characterize gibbons swinging motion [14]. With the added wrist mechanism, it allows the brachiator to turn and change axis. We then experiment with different actuators until one met the requirements.

Moreover, this research has potential influence in various industries. Especially, it can be used in the maintenance process of power transmission towers. If successful, the usage of the robotic brachiators may help avoid sending humans to elevated levels risking their lives. Another application it can impact is investigating and maintaining bridges. The proposed design can swing and climb lattice structures where bridges would need inspections regularly.

1. Limitations

The performed experiment was necessary to validate our torque calculations. The motor selection was depending on that experiment; however, a better yet more qualified set-up for the experiment would be recommended to collect more accurate results. For instance, a larger motor spool and rubber gourmet to ensure the maintenance of the string's position. A rigid setup is also recommended to protect the motor from moving.

2. Future work

A brachiator with the ability to swing among a slope line and change axis will highly add value to this research topic. The proposed controller in [15] will be implemented and applied to the current model.

In addition to that, using a lighter material such as carbon fiber will greatly impact the mechanism. Moreover, flexible linkages could also replace the aluminum bars, which will revolute the design to a more durable yet more reliable robot to brachiate.

VIII. REFERENCES

- [1] M. Thüring and S. Mahlke. "Usability, aesthetics and emotions in human-technology interaction." *International journal of psychology* 42.4 pp. 253-264. 2007.
- [2] L. Takayama, W. Ju, and C. Nass. "Beyond dirty, dangerous and dull: what everyday people think robots should do." 2008 3rd ACM/IEEE International Conference on Human-Robot Interaction (HRI). IEEE, 2008.
- [3] United States Department of Labor, Commonly Used Statistics.
- [4] "Bridges." ASCE's 2017 Infrastructure Report Card.
- [5] T. Rakha and A. Gorodetsky. "Review of Unmanned Aerial System (UAS) applications in the built environment: Towards automated building inspection procedures using drones." *Automation in Construction* 93, pp.252-264. 2018.
- [6] J. R. Usherwood and J. E. Bertram, "Understanding brachiation: insight from a collisional perspective," *Journal of Experimental Biology*, vol. 206, no. 10, pp. 1631-1642, 2003.
- [7] T. Libby, T. Y. Moore, E. Chang-Siu, D. Li, D. J. Cohen, A. Jusufi, and R. J. Full, "Tail-assisted pitch control in lizards, robots and dinosaurs," *Nature*, vol. 481, no. 7380, pp. 181-184, 2012.
- [8] A. Lo, et al. "Model-Based Design and Evaluation of a Brachiating Monkey Robot with an Active Waist." *Applied Sciences* 7.9, pp. 947. 2017.
- [9] T. Fukuda and Y. Hasegawa, "Mechanism and control of mechatronic system with higher degrees of freedom," *Annual reviews in control*, vol. 28, no. 2, pp. 137-155, 2004.
- [10] J. P. Huissoon and D. Wang. "On the design of a direct drive 5-bar-linkage manipulator." *Robotica* 9.4, pp. 441-446. 1991.

- [11] J. Nakanishi, A. Radulescu, D. J. Braun, S. Vijayakumar "Spatio-temporal stiffness optimization with switching dynamics." *Autonomous Robots*. 41(2): pp. 273-91. 2017.
- [12] Alaneme, K. K., and M. O. Bodunrin. "Corrosion behavior of alumina reinforced aluminium (6063) metal matrix composites." *Journal of Minerals and Materials Characterization and Engineering* 10.12, pp.1153. 2011.
- [13] Siddiqui, Rafiq A., Hussein A. Abdullah, and Khamis R. Al-Belushi. "Influence of aging parameters on the mechanical properties of 6063 aluminium alloy." *Journal of Materials Processing Technology* 102.1-3 pp. 234-240. 2000.
- [14] F. Michilsens, K. D'Août, and P. Aerts, "How pendulum-like are siamangs? energy exchange during brachiation," *American journal of physical anthropology*, vol. 145, no. 4, pp. 581–591, 2011.
- [15] K.D. Nguyen and Dikai Liu, "Robust Control of a Brachiating Robot," *IEEE/RSJ International Conference on Intelligent Robots and Systems (IROS2017)*, Vancouver, Canada, Sep. 2017.